Cyclin A2 localises in the cytoplasm at the S/G2 transition to activate Plk1

Helena Silva Cascales[1], Kamila Burdova[2], Erik Müllers[1#], Henriette Stoy[1], Patrick von Morgen[2], Libor Macurek[2], Arne Lindqvist[1*]

*Corresponding author:
Arne Lindqvist
Department of Cell and Molecular Biology
Karolinska Institutet
Stockholm, Sweden
Phone: +46-8-52487309
E-mail: arne.lindqvist@ki.se

Affiliations
1. Department of Cell and Molecular Biology; Karolinska Institutet; Stockholm, Sweden.
Current address: Discovery Sciences, AstraZeneca R&D; Gothenburg, Mölndal, Sweden.
2. Laboratory of Cancer Cell Biology; Institute of Molecular Genetics; Academy of Sciences of the Czech Republic; Prague, Czech Republic.

Running title: Cytoplasmic Cyclin A2 at S/G2 transition

Keywords: Cyclin A2, Plk1, Bora, Cell cycle, DNA damage, Cdk1, Cdk2, p21,

Summary statement

Cyclin A2 localises in the cytoplasm at completion of DNA replication, suggesting a mechanism for coupling S-phase with activation of the mitotic kinase Plk1

Abstract

Cyclin A2 is a key regulator of the eukaryotic cell cycle. By forming complexes with Cdk1 and Cdk2, Cyclin A2 regulates both spatial and temporal phosphorylation of target proteins, particularly during S and G2 phases. Here we describe a change in localisation of Cyclin A2 from being only nuclear to both nuclear and cytoplasmic at the S/G2 border. Inflicting DNA damage in G2 phase led to a complete loss of cytoplasmic Cyclin A2 in a manner that depended on p53 and p21. In the absence of externally induced DNA damage, $p21^{-/-}$ cells showed increased cytoplasmic localisation of Cyclin A2. In addition, depletion of Cdk1 delayed accumulation of cytoplasmic Cyclin A2, suggesting that the combined action of Cdk1 and p21 can modulate Cyclin A2 localisation. Interestingly, Cyclin A2 localisation change occurs simultaneously with Plk1 kinase activation, and we provide evidence that cytoplasmic Cyclin A2 can activate Plk1. We propose that cytoplasmic appearance of Cyclin A2 at the S/G2 transition could function as the long sought for trigger for mitotic kinase activation.

52 **Introduction**

53

54 Correct progression through the cell cycle depends on the tight regulation of Cyclin-Cdk
55 complexes over time. Sequential waves of Cyclin dependent kinase (Cdk) activity ensure
56 timely phosphorylation of a large amount of substrates. Cyclins are key elements to provide
57 target specificity and affinity to Cdks. Both Cyclin A2 (CycA2) and Cyclin B1 (CycB1) have
58 been widely studied due to their involvement in progression from S phase through G2 and
59 mitosis (Morgan, 2007). However, the specific functions and regulation of CycA2 still remain
60 largely unknown.

61

62 Lack of CycA2 leads to early embryonic lethality, suggesting a critical role for CycA2 in cell
63 cycle regulation (Kalaszczynska et al., 2009; Liu et al., 1998; Murphy et al., 1997). Due to its
64 presence during S, G2, and early mitosis, CycA2 is at a strategic position to control a large
65 part of the cell cycle (Fung et al., 2007; Pagano et al., 1992; Woo and Poon, 2003). Whereas
66 CycA2 predominately associates with Cdk2 during S phase, association with Cdk1 increases
67 during the late cell cycle, suggesting that CycA2 can play multiple roles depending on cell
68 cycle stage (Merrick et al., 2008). Indeed, CycA2 regulates multiple aspects of S-phase,
69 including phosphorylation of the prereplication complexes (Furuno et al., 1999; Katsuno et
70 al., 2009), phosphorylation of components of the replication machinery (Cardoso et al.,
71 1993; Frouin et al., 2005), and phosphorylation of Cdc6 to prevent re-replication (Petersen
72 et al., 1999). However, depletion of CycA2 primarily leads to an arrest in G2 phase,
73 suggesting that progression through G2 phase is a key function for CycA2 (Bloom and Cross,
74 2007; De Boer et al., 2008; Fung et al., 2007; Gong and Ferrell, 2010; Gong et al., 2007;
75 Oakes et al., 2014).

76

77 During G2 phase, CycA2 stimulates transcription and represses degradation of multiple
78 mitotic regulators (Hein and Nilsson, 2016; Laoukili et al., 2008; Lukas et al., 1999; Oakes et
79 al., 2014). As the mitotic regulators accumulate, CycA2 participates in the feedback-loops
80 that culminate in full CycB1-Cdk1 activation and mitotic entry (Mitra and Enders, 2004). A
81 key player in these feedback-loops is Polo-like kinase 1 (Plk1) (Lindqvist et al., 2009). Plk1
82 requires Cdk-mediated phosphorylation of the co-factor Bora for activation, and both CycA2-
83 and CycB1-containing complexes have been suggested to phosphorylate Bora (Gheghiani et
84 al., 2017; Parrilla et al., 2016; Thomas et al., 2016).

85 As CycA2 functions in both S and G2 phases, how S-phase and G2-phase targets are
86 temporally separated remains unclear. Interestingly, although at least S-phase CycA2 targets
87 are predominately nuclear, CycA2 has been shown to regulate events in the cytoplasm. This
88 includes G2 roles as loading Eg5 to centrosomes (Kanakkanthara et al., 2016) and inhibiting
89 endocytic vesicle fusion to control membrane transport as cells enter into mitosis
90 (Woodman et al., 1993). Recently, CycA2 has been reported to regulate cell motility and
91 invasiveness by interacting with RhoA (Arsic et al., 2012; Bendris et al., 2014). Thus, CycA2
92 has both nuclear and cytoplasmic functions.
93
94 Despite being predominantly nuclear and not possessing a classical NLS, CycA2 is known to
95 shuttle between the nucleus and cytoplasm to act on both nuclear and cytoplasmic
96 substrates (Jackman et al., 2002). In turn, CycA2 association with different proteins may
97 affect localisation both to the nucleus and to the cytoplasm (Maridor et al., 1993; Tsang et
98 al., 2007). However the exact mechanism that regulates CycA2 localisation remains elusive.
99
100 In order to study the localisation of Cyclin A2 in the human cell cycle we used gene-targeting
101 to create a fusion between Cyclin A2 and YFP. Here we describe the cell cycle-dependent
102 localisation of CycA2 in the cytoplasm at the S/G2 transition. We further describe that
103 cytoplasmic localisation of CycA2 is abolished in response to DNA damage in a manner that
104 depends on p21. Although our data indicate that additional modes of regulation likely exist,
105 we show that Cdk1 and p21 can act in a collaborative manner to modulate CycA2
106 localisation. Finally, we show that CycA2 interacts with Bora in the cytoplasm and
107 contributes to Plk1 activation at the S/G2 transition.
108
109

110 ## Results

111 **Cyclin A2 accumulates in the cytoplasm at the S/G2 transition**

112 In order to study the dynamics of CycA2 in live cells we targeted *CCNA2* using rAAV-
113 mediated homologous recombination. We introduced an ORF for EYFP in the *CCNA2* locus of
114 U2OS (Akopyan et al., 2014) and RPE cell lines to create a CycA2-eYFP fusion protein (Figs.
115 1A and S1A,B). Western blot analysis confirmed the successful integration of the EYFP ORF in
116 one of the two alleles of CycA2 as we detected a band that migrated at the predicted size of
117 endogenous untagged CycA2 and a band that migrated at the predicted size of the CycA2-
118 eYFP fusion protein (Fig. S1A). Importantly, siRNA to target CycA2, addition of S-trityl-L-
119 cysteine (STLC), or addition of etoposide showed a similar behaviour of both bands as to
120 CycA2 in parental RPE cells, indicating that eYFP was specifically introduced at the *CCNA2*
121 locus (Fig. S1A). As previously described, CycA2-eYFP is present in all cells from the
122 beginning of S phase and its levels increase over time reaching a maximum at mitosis when
123 CycA2 is rapidly degraded (Figs. 1A and S1B) (Akopyan et al., 2014).
124
125 Time-lapse imaging of gene-targeted U2OS and RPE cells revealed the presence of CycA2-
126 eYFP in the cytoplasm in all cells before entry into mitosis (Figs. 1A and S1B). We traced
127 individual RPE-CycA2-eYFP cells and quantified the YFP intensity both in the nucleus and the
128 cytoplasm (Fig. 1B). We observed a nuclear CycA2-eYFP increase over time reaching a
129 maximum at mitosis. Interestingly we also observed a dip in the nuclear signal starting 4 to 6
130 hours before mitosis, concomitant with an increase in the cytoplasmic signal of CycA2-eYFP.
131 The reduction of nuclear CycA2-eYFP when cytoplasmic CycA2-eYFP appears could indicate
132 that CycA2 is translocated from the nucleus to the cytoplasm. Nonetheless, both the nuclear
133 decrease and the cytoplasmic increase of CycA2-eYFP were consistent in all cells that
134 entered mitosis, indicating that CycA2-eYFP localisation change is a cell cycle regulated
135 event (Fig. 1B).
136
137 In order to pinpoint the position in the cell cycle when cells start to accumulate cytoplasmic
138 CycA2, we treated RPE CycA2-eYFP cells with a short pulse of EdU to mark cells in S phase
139 and stained with antibodies against GFP to detect CycA2-eYFP and DAPI to measure the DNA
140 content. Quantification of the stainings showed that whereas CycA2-eYFP is present in the
141 nucleus from early S-phase, cells positive for cytoplasmic CycA2-eYFP contain 4n DNA
142 content and low EdU staining, indicating that accumulation of CycA2-eYFP occurs in G2
143 phase (Fig. 1C). We next performed a similar analysis on parental untagged RPE cells, using

144 an antibody to detect endogenous CycA2. Again, we could observe that the majority of cells
145 positive for cytoplasmic CycA2 show a G2 DNA content and low EdU staining (Fig. 1D).
146 However, we note that CycA2-eYFP showed a slightly higher expression in the cytoplasmic
147 fraction compared to CycA2 (Fig. 1E). Indeed, the presence of an EYFP could alter the
148 dynamics of the endogenous protein (Snapp, 2005). Importantly however, although the
149 magnitude of cytoplasmic accumulation may differ, the timing of cytoplasmic appearance is
150 similar for CycA2 and CycA2-eYFP, showing that CycA2-eYFP can be used to study CycA2
151 localisation (Figs. 1C,D).
152
153 In both parental and CycA2-eYFP RPE cells, a subset of cells containing cytoplasmic CycA2
154 were positive for EdU, likely reflecting the time difference between EdU addition and
155 fixation of the cells (Figs. 1C,D). This indicates that CycA2 appears in the cytoplasm
156 immediately after completion of S-phase, 4-6h before mitosis (Figure 1B-D). To detect
157 whether cytoplasmic accumulation of CycA2-eYFP depends on completion of S-phase, we
158 treated RPE-CycA2-eYFP cells with thymidine or hydroxyurea and quantified the amount of
159 cells that accumulate CycA2-eYFP in the cytoplasm (Fig. 1F). The treatment with either drug
160 resulted in a decreased number of cells accumulating CycA2 in the cytoplasm, suggesting
161 that cells blocked in S phase do not gain cytoplasmic CycA2-eYFP, further indicating that
162 CycA2-eYFP starts to localise in the cytoplasm at the S/G2 transition.
163
164 **Cyclin A2-eYFP cytoplasmic appearance after modulation of Cdk activity**
165 The observation that CycA2-eYFP only accumulates in the cytoplasm after S-phase
166 completion suggests that cytoplasmic accumulation is suppressed during S-phase or
167 stimulated during G2 phase. We previously showed that mitotic-inducing activities of Cdk1
168 and Plk1 start to accumulate at the S/G2 transition (Akopyan et al., 2014). However, we find
169 no evidence that addition of inhibitors to Plk1 or its upstream kinase Aurora A affects
170 cytoplasmic appearance of CycA2 (not shown). Addition of inhibitors to Cdk1 or Cdk2 led to
171 a slight decrease in cells accumulating cytoplasmic CycA2-eYFP, but interpretation of these
172 results is hampered by that Cdk inhibition may affect S-phase progression (not shown). To
173 this end, we followed individual cells that had a low but clear presence of CycA2-eYFP in the
174 cytoplasm at the time of addition of inhibitors. To improve comparison, we synchronised
175 these cells *in silico* at the time point when each cell reaches a certain level of cytoplasmic
176 CycA2-eYFP (Fig. S2A). This allowed us to assess the contribution of Cdk1/2 activity to the
177 cytoplasmic localisation of CycA2-eYFP specifically in G2 phase. We did not observe

178 significant differences in the dynamics of cytoplasmic accumulation of CycA2-eYFP in either
179 of the treatments, showing that a reduction of Cdk1/2 activity does not compromise
180 cytoplasmic accumulation of CycA2-eYFP once initiated (Fig. S2A).
181
182 To test if Cdk1/2 activity could promote the onset of cytoplasmic accumulation of CycA2-
183 eYFP, we increased Cdk activity using a Wee1 inhibitor. Wee1 inhibition increased the
184 amount of mitotic cells and decreased the duration between cytoplasmic appearance of
185 CycA2-eYFP and mitotic entry, suggesting that Cdk activity is increased and that G2 phase is
186 shortened. However, we did not detect an increased rate of cytoplasmic appearance of
187 CycA2-eYFP after Wee1 inhibition (Fig. S2B). Thus, although Cdk1/2 activity cannot be
188 excluded as a regulator of CycA2 localisation, other components likely play a more decisive
189 role in this process.
190
191 **Cdk1 can contribute to cytoplasmic accumulation of Cyclin A2**
192 Given the lack of evidence for key G2 kinase activities to modulate CycA2 localisation, we
193 reasoned that perhaps a change in binding partner could explain CycA2 cytoplasmic
194 localisation. CycA2 is described to complex predominately with Cdk2 in S-phase and
195 increasingly with Cdk1 as cells approach mitosis (Merrick et al., 2008). Furthermore, while
196 Cdk2 is mostly nuclear, Cdk1 is present both in the nucleus and cytoplasm (Moore et al.,
197 1999; Pines and Hunter, 1991, 1994), therefore potentially providing a mechanism to
198 regulate CycA2 localisation.
199
200 To investigate the involvement of Cdk-Cyclin complex formation in the localisation of CycA2
201 we used siRNAs to target either Cdk1 or Cdk2 (Fig. 2A). Live-cell imaging of RPE CycA2-eYFP
202 cells after Cdk1 or Cdk2 knockdown revealed reduced numbers of cells going through
203 mitosis. Further, Cdk1 knockdown increased mitotic duration, showing that knockdown of
204 either Cdk affected cell cycle progression (Fig. 2B). We transfected either Cdk1 or Cdk2
205 siRNAs for 48 h, fixed cells after treating them with a short pulse of EdU, and stained using
206 CycA2 antibodies and DAPI (Fig. 2C). Analysis of quantitative immunofluorescence in single
207 cells revealed that knock down of Cdk1 led to an increase in the number of cells in G2,
208 presumably due to a lengthening of G2 phase, and subsequently, to the amount of cells with
209 cytoplasmic CycA2 (Fig. 2C,D). Interestingly, a subset of G2 cells contained high nuclear
210 CycA2 and low cytoplasmic CycA2 levels, indicating that Cdk1 may facilitate the localisation
211 of CycA2 to the cytoplasm (Fig. 2C, arrows; Fig. 2D, grey triangle). On the other hand, Cdk2

212 knockdown led to a marked decrease in number of cells in G2 phase, explaining the reduced
213 level of CycA2 and Cdk1 on a population level (Fig. 2A,C, and D). However, contrary to the
214 observation after Cdk1 depletion, the relation between nuclear and cytoplasmic CycA2 was
215 similar after Cdk2 and control knockdown (Fig. 2D). This suggests that Cdk1 influences the
216 cytoplasmic accumulation of CycA2. We therefore sought to test if Cdk1 binds to cytoplasmic
217 CycA2 and Cdk2 binds to nuclear CycA2. To this end, we immunoprecipitated CycA2-eYFP
218 from cytosolic and nuclear fractions and probed for Cdk1 or Cdk2. We find that although the
219 distribution may differ somewhat, both Cdk1 and Cdk2 are present in both nuclear and
220 cytoplasmic CycA2-eYFP immunoprecipitates (Fig. 2E). Thus, our data suggest that Cdk1 is
221 involved in cytoplasmic localisation of CycA2, but also that cytoplasmic CycA2 exists in
222 complex with Cdk2, showing that cytoplasmic appearance of CycA2 cannot be explained
223 solely by association with Cdk1.
224
225 **DNA damage response modulates cytoplasmic accumulation of CycA2**
226 We next sought to test if activities present during S-phase retain CycA2 in the nucleus. S
227 phase progression is associated with a low degree of activation of the DNA damage response
228 (Petermann and Caldecott, 2006). We hypothesised that the DNA damage response could
229 directly or indirectly inhibit CycA2 cytoplasmic localisation during S phase. Indeed, addition
230 of Etoposide or Neocarzinostatin, two compounds that cause double strand DNA breaks,
231 resulted in nuclear accumulation of CycA2-eYFP in G2 cells, suggesting that CycA2
232 localisation is regulated by the DNA damage response (Fig. 3A and not shown). The loss of
233 cytoplasmic CycA2-eYFP was accompanied by an increase in nuclear CycA2-eYFP levels
234 suggesting that upon DNA damage CycA2 is translocated into the nucleus (not shown). A few
235 hours after loss of CycA2-eYFP in the cytoplasm, CycA2-eYFP signal disappeared also from
236 the nucleus (Fig. 3A). The loss of cytoplasmic CycA2-eYFP occurred at similar time-scales
237 after DNA damage as what we and others previously described for p53 and p21-dependent
238 nuclear translocation of CycB1-eYFP (Krenning et al., 2014; Mullers et al., 2014). We
239 therefore wondered if p21 or p53 play a role in the regulation of CycA2 localisation after
240 DNA damage. To this end, we transfected cells with either p21 or p53 siRNAs for 48 h and
241 assessed the dynamics of CycA2-eYFP upon DNA damage. Interestingly, p21 and p53
242 knockdown impaired both the cytoplasmic and subsequent nuclear loss of CycA2-eYFP, p53
243 knockdown being the most evident with less than 40 % of cells losing cytoplasmic CycA2 (Fig.
244 3B, left). Similarly, cells expressing only nuclear CycA2-eYFP at the time-point of addition of
245 Etoposide retained nuclear CycA2-eYFP after p21 or p53 knockdown (Fig. 3B, right).

246 Altogether, these results suggest that p21 and p53 regulate CycA2 localisation and protein
247 levels upon DNA damage.
248
249 **p21 can modulate CycA2 localisation to the cytoplasm**
250 Given the indications of p21 and p53 playing a role in CycA2 localisation upon DNA damage,
251 we decided to further explore their contribution to CycA2 regulation in unperturbed
252 conditions. To do so we used CRISPR/Cas9 to establish p21 or p53 deficient RPE cell lines
253 (Fig. S3A). We imaged $p21^{-/-}$, $p53^{-/-}$, and WT RPE cells and recorded the cumulative mitotic
254 entry of each cell line. The three cell-lines entered mitosis at a similar rate, indicating that
255 these cell lines show no major differences in proliferation (Fig. S3B). Next, we fixed cells
256 after a short pulse with EdU, stained using DAPI and antibodies against CycA2, and
257 quantified the levels of nuclear and cytoplasmic CycA2 in S or G2 phase (Fig. 4A). We
258 observed that both $p21^{-/-}$ and $p53^{-/-}$ cell lines accumulated nuclear CycA2 similar to the WT
259 cell line (Fig. 4B). However, quantification of cytoplasmic CycA2 revealed that p21 deficiency
260 led to an increase in cytoplasmic CycA2 in both S and G2 phase (Fig. 4B). To a lower extent,
261 we also detect increased cytoplasmic CycA2 staining in $p53^{-/-}$ G2 cells. Finally, we
262 immunoprecipitated CycA2 YFP from cells synchronized in G2 and found that it specifically
263 interacted with p21 in both cytosolic and nuclear fractions (Fig. 2E). Combined, our results
264 indicate that p21 negatively regulates cytoplasmic localisation of CycA2 both in the presence
265 and absence of externally induced DNA damage.
266
267 **CycA2 triggers Plk1 activation at the S/G2 transition**
268 The cytoplasmic appearance of CycA2 at the S/G2 transition coincides with activation of Plk1
269 and Cdk1, raising the possibility that these events are linked (Akopyan et al., 2014). We find
270 that Cdk1 or Plk1 inhibition does not impede CycA2 appearance in cytoplasm, suggesting
271 that CycA2 localisation change is not downstream of mitotic kinase activation (Fig. 2A). To
272 test whether CycA2 is required for Plk1 activation, we depleted CycA2 by siRNA and
273 monitored S-phase progression by a PCNA chromobody and Plk1 activation by a FRET-based
274 biosensor (Akopyan et al., 2014). Whereas control cells show Plk1 activation as PCNA foci
275 sharply decrease at the S/G2 border, CycA2 depleted cells showed no sharp decrease in
276 PCNA foci. Rather, the amount and intensity of PCNA foci gradually decreased, and Plk1
277 activity remained low (Fig. 5A, B). This shows that Plk1 activation is impaired after CycA2
278 depletion, but also suggests that the S/G2 transition is impaired in the absence of CycA2. To
279 assess whether Cyclin-Cdk complexes affected Plk1 activity after completion of the S/G2

transition, we next added inhibitors to Cdk1 and Cdk2 to G2 cells. We find that addition of either Cdk1 or Cdk2 inhibitor disturbed Plk1 activity as well as the pT210 modification of PLK1, showing the most prominent effect with a combination of both inhibitors (Fig. 5C, 5D). Thus, both CycA2 RNAi and addition of Cdk inhibitor impairs Plk1 activation, suggesting that CycA2 stimulates Plk1 activation.

We and others previously showed that Plk1 is activated by Aurora A, in a reaction that requires the cofactor Bora (Macurek et al., 2008; Seki et al., 2008). In addition, Bora is heavily phosphorylated by CycB1-Cdk1 at mitotic entry, and the integrity of these phosphorylation sites is important for Plk1 activation (Parrilla et al., 2016; Tavernier et al., 2015; Thomas et al., 2016). Here we find that the Aurora A-mediated phosphorylation of Plk1 was further stimulated by CycA2-Cdk2 activity in the presence of Bora, suggesting that similarly as CycB1-Cdk1, also CycA2-Cdk2 can stimulate activation of Plk1 (Figure 5E) (Gheghiani et al., 2017). To assess if and where CycA2 forms a complex with Plk1 and Bora, we immunoprecipitated CycA2 from nuclear or cytoplasmic extracts of G2 cells and probed for interactors. Cdk1 and Cdk2 co-immunoprecipitated with CycA2 from both nuclear and cytoplasmic extracts, suggesting that CycA2-Cdk1 and CycA2-Cdk2 are present throughout the cell (Figure 2E). Interestingly however, we found that both Bora and Plk1 co-immunoprecipitated with CycA2 specifically in the cytoplasm (Figure 5F). Thus, although Plk1 is active in both nucleus and cytoplasm and Plk1 is in close proximity to CycA2 in both compartments (Figure S4), the activating interaction involving Bora occurs in the cytoplasm. Taken together, our results suggest that cytoplasmic CycA2 plays a key role in activating Plk1.

307 **Discussion**

308 Here we show that CycA2 appears in the cytoplasm at the S/G2 transition. We find that
309 cytoplasmic localization of CycA2 depends on at least two principal components. First, we
310 find that association with Cdk1 stimulates cytoplasmic appearance of CycA2. Second, we find
311 that p21 restricts cytoplasmic CycA2. Both these components are likely complemented by
312 additional mechanisms, as we detect cytoplasmic CycA2 in complex with Cdk2 and p21-
313 negative cells with limited amounts of cytoplasmic CycA2. Although p21 expression occurs
314 independently of p53 in the absence of induced DNA damage, p21 levels in S phase are
315 generally low due to DNA-replication dependent degradation (Kim et al., 2008; Macleod et
316 al., 1995; Nishitani et al., 2008). It therefore remains a possibility that p21, rather than
317 keeping CycA2 nuclear during an unperturbed S-phase, functions as a safety mechanism that
318 restricts cytoplasmic appearance of CycA2 in case of premature positive stimulus.
319
320 The regulated appearance of CycA2 in the cytoplasm at the S/G2 transition suggests that
321 CycA2 can direct Cdk activity both in a temporal and spatial manner. This is similar to CycB1,
322 whose change in localisation just prior to mitosis provides access to nuclear substrates
323 (Pines and Hunter, 1991). We identify Bora as a substrate for CycA2 in the cytoplasm,
324 indicating that CycA2 appearance in cytoplasm links to activation of Plk1. Given that multiple
325 cytoplasmic targets of CycA2 have been described, and that Cdk2 is identified as a major
326 interaction hub in the cytoskeleton, we note the possibility that other processes are
327 differentially regulated before and after completion of S-phase (Arsic et al., 2012; Bendris et
328 al., 2014; Kanakkanthara et al., 2016; Thul et al., 2017; Tsang et al., 2007; Woodman et al.,
329 1993).
330
331 A long standing idea in the cell cycle field has been that upon stress, cell cycle progression
332 can be delayed by altering the localisation of key proteins as Cdc25B, Cdc25C, and Cyclin B1
333 (Takizawa and Morgan, 2000). Recently, we and others showed that upon DNA damage,
334 terminal cell cycle exit from G2 phase is marked by a p21-dependent abrupt translocation of
335 Cyclin B1 to the nucleus (Krenning et al., 2014; Mullers et al., 2014). Here we found that
336 after DNA damage, CycA2 localised to the nucleus. Similarly to CycB1, the DNA-damage
337 dependent nuclear localisation of CycA2 depended on p53 and p21 (Krenning et al., 2014;
338 Mullers et al., 2014). Interestingly, early after DNA damage a low level of Cdk activity is
339 sustained and Bora remains associated with Plk1 (Bruinsma et al., 2017; Mullers et al.,

340 2017). This opens up the possibility that CycA2-dependent cytoplasmic functions can be
341 retained early during a DDR.
342
343 The S/G2 transition is marked by an increase in Cdk1 and Plk1 activities, which through
344 feedback loops slowly build up until enforcing mitotic entry (Akopyan et al., 2014). Whereas
345 Plk1 increases Cdk1 activity by phosphorylation of Wee1 and Cdc25, Plk1 activation requires
346 Cdk-dependent phosphorylation of the Plk1 interactor Bora (Parrilla et al., 2016; Tavernier et
347 al., 2015; Thomas et al., 2016). How to separate the hen from the egg and identify a starting
348 point in these feedback loops has remained an unsolved question, but several studies have
349 suggested a role for CycA2 as an initiating activity (De Boer et al., 2008; Fung et al., 2007;
350 Gheghiani et al., 2017; Gong et al., 2007; Mitra and Enders, 2004). However, CycA2-Cdk2
351 activity is present during S-phase, raising the question why Plk1 activation is detected at the
352 S/G2 transition (Akopyan et al., 2014; Spencer et al., 2013). Interestingly, whereas proteins
353 as Plk1 and CycB1-Cdk1 are both nuclear and cytoplasmic, Bora appears exclusively
354 cytoplasmic (Bruinsma et al., 2015; Feine et al., 2014).
355
356 We propose a model in which the rising cytoplasmic activity of CycA2-Cdk initiates activation
357 of Plk1 through phosphorylation of the cytoplasmic cofactor Bora (Fig. 6). Late in G2,
358 combined activities of CycA2-Cdk and CycB-Cdk1 further increase activation of Plk1 through
359 massive modification of Bora, eventually resulting in commitment to mitosis and protection
360 of Bora from SCF-dependent degradation (Feine et al., 2014; Gheghiani et al., 2017;
361 Tavernier et al., 2015; Thomas et al., 2016). We find no evidence that Cdk1 or Plk1 activities
362 influence CycA2 localisation, supporting the idea that rather than a component of feedback
363 loops, CycA2 appearance in the cytoplasm functions as a trigger for mitotic kinase activation.
364
365 **Acknowledgements**
366 We thank the members of Lindqvist and Macurek labs for comments and suggestions. This
367 work was supported by grants from the Swedish Research Council, the Swedish Foundation
368 for Strategic Research, the Swedish Cancer Society and the Grant Agency of the Czech
369 Republic (17-04742S).
370
371
372

373 ## Materials and Methods

374 **Cell culture**

375 Human hTERT-RPE1 (hereafter referred to as RPE), U2OS and HeLa cells were cultured in an
376 ambient-controlled incubator at 37°C and 5% CO_2. All cells were a kind gift from René
377 Medema and were regularly controlled for mycoplasma infection. RPE cells were cultured
378 using DMEM-F12 + GlutaMAX (Invitrogen) supplemented with 10% heat-inactivated FBS
379 (HyClone) and 1% P/S (HyClone). U2OS and HeLa cells were cultured using DMEM +
380 GlutaMAX (Invitrogen) supplemented with 6% heat-inactivated fetal bovine serum (FBS,
381 HyClone) and 1% Penicillin/Streptomycin (P/S, HyClone). For adeno-associated virus
382 production, HEK293 cells were cultured using DMEM + GlutaMAX (Invitrogen) supplemented
383 with 10% heat-inactivated fetal bovine serum (FBS, HyClone) and 1% Penicillin/Streptomycin
384 (P/S, HyClone). For live-cell imaging experiments the medium of the cells was changed to
385 Leibowitz-15 (Invitrogen) supplemented with 10% FBS (HyClone) and 1% P/S (HyClone) at
386 least 12h before initiation of the imaging.

387

388 **Establishment of cell lines**

389 RPE CycA2-eYFP cells were obtained by adeno-associated (AAV)-mediated homologous
390 recombination as previously described (Akopyan et al., 2014). Briefly, the targeting cassette
391 was designed to contain an arm of 1.1 kb of homology with the sequence directly 5' of the
392 *CCNA2* Stop codon followed by the ORF of EYFP and another arm of homology 1.016 kb with
393 the 3' UTR of the *CCNA2* gene. Adeno-associated viruses containing the homology cassette
394 were produced and used to transduce RPE cells. Four days after transduction cells were
395 sorted by FACS to enrich the YFP-positive population. After two rounds of sorting, single YFP
396 positive cells were seeded in 96-well plates and clones which were validated by Western
397 blot and live-cell imaging. Knock out of *TP53* and *p21* in RPE cells using CRISPR/Cas9 was
398 generated as described previously (Pechackova et al., 2016) and independent clones were
399 validated by western blotting and sequencing of the genetic loci.

400

401 **Cell synchronization**

402 RPE or RPE CycA2-eYFP cells were synchronized in G0 by growing to confluency, split to fresh
403 medium supplemented with thymidine (2 mM) and grown for 40 h. Cells were released to
404 fresh medium and collected after 5h. Synchronization efficiency was validated by flow
405 cytometry using 4n DNA content and absence of pS10-H3 staining as G2 markers. Typically,
406 this protocol yielded >95% G2 population and less than 0.5 % mitotic cells.

407

408 **Cell fractionation and Immunoprecipitation**

409 Cells were fractionated using hypotonic lysis as previously described (Andersen et al., 2002).
410 Briefly, cells were collected by trypsinization and centrifugation (300 *g* for 5 min at 4°C), and
411 washed with PBS. The cell pellet was resuspended in 5× packed cell volume of hypotonic
412 buffer A (10 mM Hepes-KOH, pH 7.9, 10 mM KCl, 1.5 mM $MgCl_2$, 0.5 mM DTT, and 0.5 mM
413 PMSF) supplemented with a cocktail of protease inhibitors (cOmplete, EDTA free; Roche)
414 and phosphatase inhibitors (PhosSTOP, Roche) and incubated on ice for 5 min. Next, the
415 cells were spun down at 500 *g* for 5 min, suspended in 2× packed cell volume of
416 supplemented buffer A and dounced using a tight-fitting pestle. Nuclei were collected by
417 centrifugation at 500 *g* for 5 min at 4°C. Supernatant was centrifuged 20000g 10 min 4°C,
418 supplemented with NaCl and Triton X-100 to 150 mM and 0.1 % final concentration,
419 respectively and used as cytoplasmic fraction. Nuclei were cleaned by centrifugation over
420 sucrose gradient, lysed in lysis buffer (10 mM HEPES pH 7.9, 10 mM KCl, 150 mM NaCl, 1.5
421 mM MgCl2, 0.1 % NP-40, 0.5mM DTT, 0.5 mM PMSF supplemented with protease inhibitor
422 cocktail and PhosSTOP), sonicated and cleared by centrifugation at 20000 g 10min 4°C. For
423 IP 2 mg of cytoplasmic and nuclear extracts were incubated with either 15 ml GFP Trap
424 beads (Chromotek) for 1 h at 4°C or 1-1.5 μg IgG overnight at 4°C, Protein A/G Ultralink
425 beads were added for last 2 h. Beads were washed four times with lysis buffer and
426 precipitates were eluted to SDS-PAGE sample buffer.

427

428 **Inhibitors**

429 For live-cell imaging and quantitative immunofluorescence experiments, the following
430 inhibitors were used at the indicated concentrations for 4 h unless indicated differently in
431 the experiments: RO-3306 at 10 μM (Cdk1 inhibitor; Calbiochem), NU6140 at 10 μM (Cdk2
432 inhibitor; Calbiochem), Roscovitine at 25 μM (broad Cdk inhibitor; Selleck Chemicals), MK-
433 1775 at 100 μM (Wee1 inhibitor; Selleck Chemicals), BI2536 at 100 nM (Plk1 inhibitor,
434 Selleck Chemicals), MLN8237 at 100nM (Aurora A inhibitor; Selleckchem), Etoposide 2μM
435 (topoisomerase II inhibitor; Sigma Aldrich), Neocarzinostatin at 2 nM (toxin; Sigma Aldrich),
436 KU60019 at 10 μM (ATM inhibitor; Tocris Bioscience), VE821 at 10 μM (ATR inhibitor;
437 Selleckchem), Cycloheximide at 10 μg/ml (inhibitor of protein synthesis; Sigma Aldrich),
438 Thymidine at 2.5 mM (Sigma Aldrich) and Hydroxyurea at 2 mM (ribonucleotide reductase
439 inhibitor; Sigma Aldrich).

440

441 **siRNA transfection**

442 SMARTpool ON-TARGET plus siRNAs targeting CycA2, Cdk1, Cdk2, p21 or p53 as well as a
443 scrambled control siRNA were purchased from Dharmacon and employed at a concentration
444 of 20nM using HiPerFect transfection reagent (Qiagen) and OptiMEM (Invitrogen) at 48h and
445 24h before live-cell imaging or fixation.

446

447 **Live-cell microscopy**

448 For live cell imaging experiments, 10.000 cells were seeded in 96-well imaging plates (BD
449 Falcon) using Leibowitz-15 medium (Invitrogen) 16 h prior to initiation of the imaging on an
450 ImageXpress system (Molecular Devices) using a 20x NA 0.45 objective. Images were
451 processed and analysed using ImageJ. Nuclei and cytoplasms were selected by manual
452 drawing. Integrated intensities were calculated for nuclei whereas an area of the cytoplasm
453 was measured and mean or median intensities were measured for cytoplasmic
454 quantifications. FRET microscopy was performed as in (Hukasova et al., 2012) and
455 simultaneous monitoring of FRET and a PCNA chromobody was performed as in (Akopyan et
456 al., 2014).

457

458 **Antibodies**

459 The following antibodies were: GFP (1:400; ab13970 abcam), Cyc A2 (1:100 #sc-751, Santa
460 Cruz), CycA2 (1:500; #4656 Cell Signalling), Plk1 (ab14210; Abcam), affinity purified mouse
461 anti pT210-Plk1 (clone K50-483, Becton Dickinson), affinity purified rabbit anti-Bora
462 (Bruinsma et al., JCS 2014), Cdk1 (sc-54, Santa Cruz and #9116 Cell Signalling), Cdk2 (sc-163,
463 Santa Cruz and #2564 Cell Signalling), GAPDH (1:5000; G9545 Sigma Aldrich), H2B (1:1000;
464 ab1790 abcam), β-Tubulin (1:500, #2128S Cell Signalling), Alexa Fluor 488-Goat anti-chicken
465 (1:1000; #A11039 Life Technologies) and Alexa Fluor 647-Donkey anti-rabbit (1:1000;
466 #A31537 Life Technologies).

467

468 **Quantitative immunofluorescence**

469 For quantitative immunofluorescence experiments 10.000 cells were seeded 16h before the
470 different treatments with inhibitors. For siRNA transfections, 5.000 cells were seeded
471 instead. Twenty minutes before fixation EdU (5-ethynyl-2'-deoxyuridine, Molecular probes)
472 was added in all the experiments. Cells were fixed using 3.7% formaldehyde (Sigma Aldrich)
473 for 5 minutes and permeabilised using -20°C methanol (Sigma Aldrich) for 2 minutes,
474 blocking was performed using 2% bovine albumin serum (BSA; Sigma Aldrich) in TBS

475 supplemented with 0.1% Tween20 (TBS-T). After blocking, cells were incubated with primary
476 antibodies at 4°C overnight. After washing, cells were incubated with secondary antibodies
477 and DAPI for 1h at room temperature. Click chemistry was performed after wash of the
478 secondary antibody using a mixture of 100mM Tris, 1mM $CuSO_4$, 100mM ascorbic acid and
479 fluorescent dye (#A10277 and #A10266, Invitrogen) and incubated for 1h at room
480 temperature. Images were acquired on an ImageXpress system (Molecular Devices) using
481 either a 20x (NA) objective or a 40x NA 0.6 objective. Images were manually screened for
482 wrong cells and processed and analysed using CellProfiler (Carpenter et al., 2006) to identify
483 and measure nuclear and cytoplasmic fluorescence intensity of single cells. Cell cycle stages
484 were determined setting a threshold both on DAPI and EdU levels.
485
486 ***In vitro* kinase assay**
487 Kinase dead Plk1-K82R, GST-Bora and GST-Aurora-A were purified from bacteria as
488 described (Macurek et al., 2008) and incubated with CycA2/Cdk2 (100 ng/reaction, Biaffin
489 GmbH) in a kinase buffer (25 mM MOPS pH 7.2, 12.5 mM glycerol 2-phosphate, 25 mM
490 MgCl2, 5 mM EGTA, 2 mM EDTA and 0.25 mM DTT) supplemented with 100 μM ATP and 5
491 μCi 32P-γ-ATP at 30°C for 30 min. After separation of proteins by SDS-PAGE, phosphorylation
492 was detected by autoradiography or by pT210-Plk1 antibody.
493
494 **Proximity ligation assay (PLA)**
495 RPE CycA2-eYFP cells were fixed for 10 min with 4 % paraformaldehyde in PBS and
496 permeabilized with 0.2 % Triton X-100 for 5 min at room temperature. Proximity ligation
497 assay (PLA) was performed using mouse anti-PLK1, rabbit anti-cyclin A antibodies and
498 Duolink reagent according to the manufacturers protocol (Sigma-Aldrich). YFP signal was
499 used to identify cells with cytoplasmic CycA2. Signal was imaged by a Leica SP5 confocal
500 microscope using 63 X oil objective.

501

502 ## Figure legends

503 **Figure 1. Cyclin A2 accumulates in the cytoplasm at the S/G2 transition**

504 (**a**) Time-lapse imaging through mitosis of a single RPE cell gene-targeted to express CycA2-
505 eYFP. Time between images is 20 minutes.

506 (**b**) Quantification of CycA2-eYFP mean intensity in the nucleus (left) and mean intensity in
507 the cytoplasm (middle) of 20 individual cells over time. Cells were synchronised *in silico* to
508 set t=0 at mitosis. The black dotted line represents the average fluorescence intensity of all
509 the cells measured. Plot of the average of nuclear and cytoplasmic mean intensity of 20 cells
510 (right).

511 (**c**) RPE CycA2-eYFP cells were incubated for 20 min with EdU and fixed. Left graphs shows
512 quantification of nuclear and cytoplasmic integrated intensity of GFP staining versus nuclear
513 DAPI intensity in at least 1500 cells; each dot represents one cell. Middle graph shows
514 nuclear versus cytoplasmic integrated intensities of GFP staining; the grey square indicates
515 the gating for expressors of both nuclear and cytoplasmic CycA2-eYFP. Right graphs show
516 integrated EdU intensity versus integrated DAPI intensity, with or without gating for
517 expressors of both nuclear and cytoplasmic CycA2-eYFP (bottom right).

518 (**d**) RPE cells were treated as in (c), with the difference that at least 1200 cells were
519 quantified and GFP antibody was replaced by CycA2 antibody.

520 (**e**) Western blot of nuclear and cytoplasmic fractions of unsynchronised RPE-CycA2-eYFP
521 cells using the indicated antibodies.

522 (**f**) Quantification of the percentage of cells accumulating CycA2-eYFP in the cytoplasm after
523 different treatments. Cells were treated with DMSO (Control), Thymidine (THY) or
524 Hydroxyurea (HU) and imaged. The number of cells accumulating CycA2 in the cytoplasm
525 was recorded and plotted as a percentage of the total number of cells tracked.
526 All experiments were repeated at least three times.

527

528 **Figure 2. Cdk1 can contribute to cytoplasmic accumulation of Cyclin A2**

529 (**a**) Western blot of cells transfected with Cdk1, Cdk2 or scrambled (Control) siRNAs for 48 h.
530 Samples were prepared from 4 wells in a 96-well plate to mimic conditions used for
531 microscopy.

532 **(b)** Amount of cells going through mitosis during 16 h after knock down of Cdk1 or Cdk2 for
533 48 h (left). Duration of mitosis in the indicated knockdown conditions (right).

534 **(c)** Cells were transfected with siRNAs for either Cdk1 or Cdk2 for 48 h, incubated with EdU
535 for 20 min and fixed. Arrows indicate G2 cells with low cytoplasmic CycA.
536 (**d**) Quantification of cytoplasmic and nuclear integrated intensities of CycA2 in at least 500
537 RPE cells imaged as in (c). Cells were gated for DAPI and EdU levels and assigned to S phase
538 (green dots) or G2 phase (red dots). Each dot represents one cell; the percentages indicate
539 the proportion of S and G2 phase cells in each condition. Numbers to right show amount of
540 cells within indicated gate and total amount of G2 cells.
541 (**e**) RPE CycA2 YFP or RPE cells were synchronized in G2, separated to cytosolic and nuclear
542 fractions and immunoprecipitated with GFP Trap (left) or with control IgG and CycA2
543 antibody (right). Proteins bound to the carrier were probed with indicated antibodies.
544 A and b were repeated twice, the remaining experiments were repeated at list three times.
545
546 **Figure 3. DNA damage and the DNA damage response can modulate cytoplasmic**
547 **accumulation of Cyclin A2-eYFP**
548 (**a**) Time-lapse images of RPE CycA2-eYFP cell treated with Etoposide (arrow). Time between
549 images is 20 minutes.
550 (**b**) Quantification of the dynamics of cytoplasmic and nuclear CycA2-eYFP after DNA
551 damage. RPE CycA2-eYFP cells were transfected with p21, p53 or control siRNAs for 48 h and
552 treated with Etoposide at t=0. Single cells were tracked over time and the time point of
553 cytoplasmic loss of CycA2-eYFP were recorded. Left graphs show at least 100 cells that
554 contained cytoplasmic CycA2-eYFP at time point of addition of Etoposide. Right graphs show
555 at least 90 cells that contained only nuclear CycA2-eYFP at time point of addition of
556 Etoposide.
557 All experiments were repeated at least three times.
558
559 **Figure 4. p21 can modulate CycA2 localisation to the cytoplasm**
560 (**a**) WT, p21-/- or p53-/- RPE cells were incubated for 20 min with EdU and fixed. Graph
561 shows quantification of integrated intensity of EdU staining versus nuclear DAPI intensity in
562 at least 1500 cells; each circle represents one cell. The large grey rectangle indicates EdU
563 positive cells and the small grey rectangle indicates EdU-negative 4N cells used for
564 quantification in b.
565 (**b**) Quantification of nuclear and cytoplasmic integrated intensity of CycA2 in WT, $p53^{-/-}$ and
566 $p21^{-/-}$ RPE cells in S-phase (top) and in G2 phase (bottom), gated as shown in a. Box plots

567 indicate 90, 75, 50, 25, and 10 percentiles. Squares indicate average value. *** indicates
568 p<0.00005, students t-test.
569 All experiments were repeated at least three times.
570
571 **Figure 5. Cytoplasmic CycA2 can activate Plk1**
572 **(a)** Time-lapse sequence of U2OS cells expressing Plk1 FRET reporter and PCNA chromobody.
573 Time points (h) are indicated in figure. Top Ctrl siRNA, bottom CycA2 siRNA.
574 **(b)** Quantification of individual cells, imaged as in (a). Red line shows 1/FRET and blue line
575 shows PCNA foci.
576 **(c)** Inhibition of Cdk activity in U2OS cells expressing Plk1 FRET reporter. Cells with
577 intermediate Plk1 FRET signal, indicative of G2 phase, were followed after addition of
578 indicated inhibitors. Graph shows average and s.e.m of at least 10 cells per condition.
579 **(d)** Inhibition of Cdk activity in RPE synchronized in G2 decrease the level of Plk1
580 phosphorylation at T210.
581 **(e)** Phosphorylation of Bora by CycA2/Cdk2 promotes modification of Plk1 at T210 mediated
582 by Aurora-A. Empty arrowhead indicates position of the kinase dead Plk1, full arrowhead
583 indicates position of Bora.
584 **(f)** Cytosolic and nuclear extracts from RPE cells synchronized in G2 were subjected to
585 immunoprecipitation with anti-CycA2 or anti-Plk1 and bound proteins were probed with
586 indicated antibodies.
587 All experiments were repeated at least three times.
588
589 **Figure 6. A model for Plk1 activation by cytoplasmic CycA2.**
590 Cytoplasmic appearance of CycA2 (cA2) at the S/G2 transition enables phosphorylation of
591 Bora (B). Phosphorylated Bora interacts with Plk1 and stimulates Aurora A (Aur A)–mediated
592 phosphorylation of Plk1 T210. This is amplified by consequent CycB1 (cB1)-mediated
593 phosphorylation of Bora.
594
595
596 **Supplementary figure 1. Characterization of CycA2-eYFP cells**
597 (**a**) Western blot of RPE and RPE CycA2-eYFP cell lines, incubated with the indicated
598 antibodies. Cells were treated with CycA2 siRNA for 24 h, STLC for 16 h, or Etoposide for 24
599 h.
600 (**b**) Time-lapse imaging of a single U2OS-CycA2-eYFP cell growing on a fibronectin-coated
601 micropattern. Images were acquired every 20 minutes.

602

603 **Supplementary figure 2. Cyclin A2-eYFP cytoplasmic appearance after modulation of Cdk**
604 **activity**

605 (**a**) Quantification of nuclear (left) and cytoplasmic (right) accumulation of CycA2-eYFP in at
606 least 17 single cells treated with DMSO (top), RO-3306 (middle) or Nu6140 (bottom) for 4
607 hours; each track represents a single cell. Cells were selected based on clear but low
608 cytoplasmic CycA2-eYFP signal at time point of inhibitor addition, and synchronised *in silico*
609 at the time point when cells reached a threshold of cytoplasmic CycA2-eYFP (indicated with
610 the grey dotted line). (Below) Average of nuclear (top lines) and cytoplasmic (bottom lines)
611 intensities. Error bars show SD.

612 (**b**) Quantification of at least 95 single RPE-CycA2-eYFP cells upon treatment with either
613 DMSO (control) or Wee1 inhibitor (MK1775). Cells were treated with the drugs and tracked
614 using live-cell imaging. Each track represents one single cell, the black dot represents the
615 first time point when cytoplasmic CycA2 can be detected and the red dot indicates mitotic
616 entry. Overlap of the cumulative appearance of cytoplasmic CycA2 in the two different
617 treatments (right).

618

619 **Supplementary figure 3. Characterization of p53 and p21 knockout cells**

620 (**a**) Parental RPE, RPE-TP53-KO and RPE-p21-KO cells were treated with etoposide for 6 h and
621 whole cell lysates were probed with indicted antibodies. Two independent clones were
622 probed for each knock-out cell line.

623 (**b**) Cumulative mitotic entry of at least 280 RPE, RPE $p53^{-/-}$, and RPE $p21^{-/-}$ cells.

624

625 **Supplementary figure 4. Proximity ligation between Cyclin A2 and Plk1**

626 RPE CycA2-eYFP cells were fixed and probed for Proximity ligation assay using mouse anti-
627 Plk1 and rabbit-anti-CycA2 antibodies. Representative image of a cell with strong
628 cytoplasmic presence of CycA2-eYFP is shown. Neighbouring cell with minimal CycA2-eYFP
629 expression indicates background signal.

630

631 **References**

632 Akopyan, K., Silva Cascales, H., Hukasova, E., Saurin, A.T., Mullers, E., Jaiswal, H., Hollman, D.A., Kops,
633 G.J., Medema, R.H., and Lindqvist, A. (2014). Assessing kinetics from fixed cells reveals activation of
634 the mitotic entry network at the S/G2 transition. Mol Cell *53*, 843-853.

635 Andersen, J.S., Lyon, C.E., Fox, A.H., Leung, A.K., Lam, Y.W., Steen, H., Mann, M., and Lamond, A.I.
636 (2002). Directed proteomic analysis of the human nucleolus. Curr Biol *12*, 1-11.

637 Arsic, N., Bendris, N., Peter, M., Begon-Pescia, C., Rebouissou, C., Gadea, G., Bouquier, N., Bibeau, F.,
638 Lemmers, B., and Blanchard, J.M. (2012). A novel function for Cyclin A2: control of cell invasion via
639 RhoA signaling. J Cell Biol *196*, 147-162.

640 Bendris, N., Cheung, C.T., Leong, H.S., Lewis, J.D., Chambers, A.F., Blanchard, J.M., and Lemmers, B.
641 (2014). Cyclin A2, a novel regulator of EMT. Cell Mol Life Sci *71*, 4881-4894.

642 Bloom, J., and Cross, F.R. (2007). Multiple levels of cyclin specificity in cell-cycle control. Nat Rev Mol
643 Cell Biol *8*, 149-160.

644 Bruinsma, W., Aprelia, M., Garcia-Santisteban, I., Kool, J., Xu, Y.J., and Medema, R.H. (2017). Inhibition
645 of Polo-like kinase 1 during the DNA damage response is mediated through loss of Aurora A
646 recruitment by Bora. Oncogene *36*, 1840-1848.

647 Bruinsma, W., Aprelia, M., Kool, J., Macurek, L., Lindqvist, A., and Medema, R.H. (2015). Spatial
648 Separation of Plk1 Phosphorylation and Activity. Front Oncol *5*, 132.

649 Cardoso, M.C., Leonhardt, H., and Nadal-Ginard, B. (1993). Reversal of terminal differentiation and
650 control of DNA replication: cyclin A and Cdk2 specifically localize at subnuclear sites of DNA
651 replication. Cell *74*, 979-992.

652 Carpenter, A.E., Jones, T.R., Lamprecht, M.R., Clarke, C., Kang, I.H., Friman, O., Guertin, D.A., Chang,
653 J.H., Lindquist, R.A., Moffat, J.*, et al.* (2006). CellProfiler: image analysis software for identifying and
654 quantifying cell phenotypes. Genome Biol *7*, R100.

655 De Boer, L., Oakes, V., Beamish, H., Giles, N., Stevens, F., Somodevilla-Torres, M., Desouza, C., and
656 Gabrielli, B. (2008). Cyclin A/cdk2 coordinates centrosomal and nuclear mitotic events. Oncogene *27*,
657 4261-4268.

658 Feine, O., Hukasova, E., Bruinsma, W., Freire, R., Fainsod, A., Gannon, J., Mahbubani, H.M., Lindqvist,
659 A., and Brandeis, M. (2014). Phosphorylation-mediated stabilization of Bora in mitosis coordinates
660 Plx1/Plk1 and Cdk1 oscillations. Cell Cycle *13*, 1727-1736.

661 Frouin, I., Toueille, M., Ferrari, E., Shevelev, I., and Hubscher, U. (2005). Phosphorylation of human
662 DNA polymerase lambda by the cyclin-dependent kinase Cdk2/cyclin A complex is modulated by its
663 association with proliferating cell nuclear antigen. Nucleic Acids Res *33*, 5354-5361.

664 Fung, T.K., Ma, H.T., and Poon, R.Y. (2007). Specialized roles of the two mitotic cyclins in somatic cells:
665 cyclin A as an activator of M phase-promoting factor. Mol Biol Cell *18*, 1861-1873.

666 Furuno, N., den Elzen, N., and Pines, J. (1999). Human cyclin A is required for mitosis until mid
667 prophase. J Cell Biol *147*, 295-306.

668 Gheghiani, L., Loew, D., Lombard, B., Mansfeld, J., and Gavet, O. (2017). PLK1 Activation in Late G2
669 Sets Up Commitment to Mitosis. Cell Rep *19*, 2060-2073.

670 Gong, D., and Ferrell, J.E., Jr. (2010). The roles of cyclin A2, B1, and B2 in early and late mitotic events.
671 Mol Biol Cell *21*, 3149-3161.

672 Gong, D., Pomerening, J.R., Myers, J.W., Gustavsson, C., Jones, J.T., Hahn, A.T., Meyer, T., and Ferrell,
673 J.E., Jr. (2007). Cyclin A2 regulates nuclear-envelope breakdown and the nuclear accumulation of
674 cyclin B1. Curr Biol *17*, 85-91.

675 Hein, J.B., and Nilsson, J. (2016). Interphase APC/C-Cdc20 inhibition by cyclin A2-Cdk2 ensures
676 efficient mitotic entry. Nat Commun *7*, 10975.

677 Hukasova, E., Silva Cascales, H., Kumar, S.R., and Lindqvist, A. (2012). Monitoring kinase and
678 phosphatase activities through the cell cycle by ratiometric FRET. J Vis Exp, e3410.

679 Jackman, M., Kubota, Y., den Elzen, N., Hagting, A., and Pines, J. (2002). Cyclin A- and cyclin E-Cdk
680 complexes shuttle between the nucleus and the cytoplasm. Mol Biol Cell *13*, 1030-1045.

681 Kalaszczynska, I., Geng, Y., Iino, T., Mizuno, S., Choi, Y., Kondratiuk, I., Silver, D.P., Wolgemuth, D.J.,
682 Akashi, K., and Sicinski, P. (2009). Cyclin A is redundant in fibroblasts but essential in hematopoietic
683 and embryonic stem cells. Cell *138*, 352-365.

684 Kanakkanthara, A., Jeganathan, K.B., Limzerwala, J.F., Baker, D.J., Hamada, M., Nam, H.J., van
685 Deursen, W.H., Hamada, N., Naylor, R.M., Becker, N.A.*, et al.* (2016). Cyclin A2 is an RNA binding
686 protein that controls Mre11 mRNA translation. Science *353*, 1549-1552.

687 Katsuno, Y., Suzuki, A., Sugimura, K., Okumura, K., Zineldeen, D.H., Shimada, M., Niida, H., Mizuno, T.,
688 Hanaoka, F., and Nakanishi, M. (2009). Cyclin A-Cdk1 regulates the origin firing program in
689 mammalian cells. Proc Natl Acad Sci U S A *106*, 3184-3189.

690 Kim, Y., Starostina, N.G., and Kipreos, E.T. (2008). The CRL4Cdt2 ubiquitin ligase targets the
691 degradation of p21Cip1 to control replication licensing. Genes Dev *22*, 2507-2519.

692 Krenning, L., Feringa, F.M., Shaltiel, I.A., van den Berg, J., and Medema, R.H. (2014). Transient
693 activation of p53 in G2 phase is sufficient to induce senescence. Mol Cell *55*, 59-72.

694 Laoukili, J., Alvarez, M., Meijer, L.A., Stahl, M., Mohammed, S., Kleij, L., Heck, A.J., and Medema, R.H.
695 (2008). Activation of FoxM1 during G2 requires cyclin A/Cdk-dependent relief of autorepression by
696 the FoxM1 N-terminal domain. Mol Cell Biol *28*, 3076-3087.

697 Lindqvist, A., Rodriguez-Bravo, V., and Medema, R.H. (2009). The decision to enter mitosis: feedback
698 and redundancy in the mitotic entry network. J Cell Biol *185*, 193-202.

699 Liu, D., Matzuk, M.M., Sung, W.K., Guo, Q., Wang, P., and Wolgemuth, D.J. (1998). Cyclin A1 is
700 required for meiosis in the male mouse. Nat Genet *20*, 377-380.

701 Lukas, C., Sorensen, C.S., Kramer, E., Santoni-Rugiu, E., Lindeneg, C., Peters, J.M., Bartek, J., and Lukas,
702 J. (1999). Accumulation of cyclin B1 requires E2F and cyclin-A-dependent rearrangement of the
703 anaphase-promoting complex. Nature *401*, 815-818.

704 Macleod, K.F., Sherry, N., Hannon, G., Beach, D., Tokino, T., Kinzler, K., Vogelstein, B., and Jacks, T.
705 (1995). p53-dependent and independent expression of p21 during cell growth, differentiation, and
706 DNA damage. Genes Dev *9*, 935-944.

707 Macurek, L., Lindqvist, A., Lim, D., Lampson, M.A., Klompmaker, R., Freire, R., Clouin, C., Taylor, S.S.,
708 Yaffe, M.B., and Medema, R.H. (2008). Polo-like kinase-1 is activated by aurora A to promote
709 checkpoint recovery. Nature *455*, 119-123.

710 Maridor, G., Gallant, P., Golsteyn, R., and Nigg, E.A. (1993). Nuclear localization of vertebrate cyclin A
711 correlates with its ability to form complexes with cdk catalytic subunits. J Cell Sci *106 (Pt 2)*, 535-544.

712 Merrick, K.A., Larochelle, S., Zhang, C., Allen, J.J., Shokat, K.M., and Fisher, R.P. (2008). Distinct
713 activation pathways confer cyclin-binding specificity on Cdk1 and Cdk2 in human cells. Mol Cell *32*,
714 662-672.

715 Mitra, J., and Enders, G.H. (2004). Cyclin A/Cdk2 complexes regulate activation of Cdk1 and Cdc25
716 phosphatases in human cells. Oncogene *23*, 3361-3367.

717 Moore, J.D., Yang, J., Truant, R., and Kornbluth, S. (1999). Nuclear import of Cdk/cyclin complexes:
718 identification of distinct mechanisms for import of Cdk2/cyclin E and Cdc2/cyclin B1. J Cell Biol *144*,
719 213-224.

720 Morgan, D.O. (2007). Cell Cycle: Principles of Control (Oxford University Press).

721 Mullers, E., Silva Cascales, H., Burdova, K., Macurek, L., and Lindqvist, A. (2017). Residual Cdk1/2
722 activity after DNA damage promotes senescence. Aging Cell *16*, 575-584.

723 Mullers, E., Silva Cascales, H., Jaiswal, H., Saurin, A.T., and Lindqvist, A. (2014). Nuclear translocation
724 of Cyclin B1 marks the restriction point for terminal cell cycle exit in G2 phase. Cell Cycle *13*, 2733-
725 2743.

726 Murphy, M., Stinnakre, M.G., Senamaud-Beaufort, C., Winston, N.J., Sweeney, C., Kubelka, M.,
727 Carrington, M., Brechot, C., and Sobczak-Thepot, J. (1997). Delayed early embryonic lethality
728 following disruption of the murine cyclin A2 gene. Nat Genet *15*, 83-86.

729 Nishitani, H., Shiomi, Y., Iida, H., Michishita, M., Takami, T., and Tsurimoto, T. (2008). CDK inhibitor
730 p21 is degraded by a proliferating cell nuclear antigen-coupled Cul4-DDB1Cdt2 pathway during S
731 phase and after UV irradiation. J Biol Chem *283*, 29045-29052.

732 Oakes, V., Wang, W., Harrington, B., Lee, W.J., Beamish, H., Chia, K.M., Pinder, A., Goto, H., Inagaki,
733 M., Pavey, S.*, et al.* (2014). Cyclin A/Cdk2 regulates Cdh1 and claspin during late S/G2 phase of the cell
734 cycle. Cell Cycle *13*, 3302-3311.

735 Pagano, M., Pepperkok, R., Verde, F., Ansorge, W., and Draetta, G. (1992). Cyclin A is required at two
736 points in the human cell cycle. EMBO J *11*, 961-971.

737 Parrilla, A., Cirillo, L., Thomas, Y., Gotta, M., Pintard, L., and Santamaria, A. (2016). Mitotic entry: The
738 interplay between Cdk1, Plk1 and Bora. Cell Cycle *15*, 3177-3182.

739 Pechackova, S., Burdova, K., Benada, J., Kleiblova, P., Jenikova, G., and Macurek, L. (2016). Inhibition
740 of WIP1 phosphatase sensitizes breast cancer cells to genotoxic stress and to MDM2 antagonist
741 nutlin-3. Oncotarget *7*, 14458-14475.

742 Petermann, E., and Caldecott, K.W. (2006). Evidence that the ATR/Chk1 pathway maintains normal
743 replication fork progression during unperturbed S phase. Cell Cycle *5*, 2203-2209.

744 Petersen, B.O., Lukas, J., Sorensen, C.S., Bartek, J., and Helin, K. (1999). Phosphorylation of
745 mammalian CDC6 by cyclin A/CDK2 regulates its subcellular localization. EMBO J *18*, 396-410.

746 Pines, J., and Hunter, T. (1991). Human cyclins A and B1 are differentially located in the cell and
747 undergo cell cycle-dependent nuclear transport. J Cell Biol *115*, 1-17.

748 Pines, J., and Hunter, T. (1994). The differential localization of human cyclins A and B is due to a
749 cytoplasmic retention signal in cyclin B. EMBO J *13*, 3772-3781.

750 Seki, A., Coppinger, J.A., Jang, C.Y., Yates, J.R., and Fang, G. (2008). Bora and the kinase Aurora a
751 cooperatively activate the kinase Plk1 and control mitotic entry. Science *320*, 1655-1658.

752 Snapp, E. (2005). Design and use of fluorescent fusion proteins in cell biology.

753 Spencer, S.L., Cappell, S.D., Tsai, F.C., Overton, K.W., Wang, C.L., and Meyer, T. (2013). The
754 proliferation-quiescence decision is controlled by a bifurcation in CDK2 activity at mitotic exit. Cell
755 *155*, 369-383.

756 Takizawa, C.G., and Morgan, D.O. (2000). Control of mitosis by changes in the subcellular location of
757 cyclin-B1-Cdk1 and Cdc25C. Curr Opin Cell Biol *12*, 658-665.

758 Tavernier, N., Noatynska, A., Panbianco, C., Martino, L., Van Hove, L., Schwager, F., Leger, T., Gotta,
759 M., and Pintard, L. (2015). Cdk1 phosphorylates SPAT-1/Bora to trigger PLK-1 activation and drive
760 mitotic entry in C. elegans embryos. J Cell Biol *208*, 661-669.

761 Thomas, Y., Cirillo, L., Panbianco, C., Martino, L., Tavernier, N., Schwager, F., Van Hove, L., Joly, N.,
762 Santamaria, A., Pintard, L.*, et al.* (2016). Cdk1 Phosphorylates SPAT-1/Bora to Promote Plk1 Activation
763 in C. elegans and Human Cells. Cell Rep *15*, 510-518.

764 Thul, P.J., Akesson, L., Wiking, M., Mahdessian, D., Geladaki, A., Ait Blal, H., Alm, T., Asplund, A., Bjork,
765 L., Breckels, L.M.*, et al.* (2017). A subcellular map of the human proteome. Science *356*.

766 Tsang, W.Y., Wang, L., Chen, Z., Sanchez, I., and Dynlacht, B.D. (2007). SCAPER, a novel cyclin A-
767 interacting protein that regulates cell cycle progression. J Cell Biol *178*, 621-633.

768 Woo, R.A., and Poon, R.Y. (2003). Cyclin-dependent kinases and S phase control in mammalian cells.
769 Cell Cycle *2*, 316-324.

770 Woodman, P.G., Adamczewski, J.P., Hunt, T., and Warren, G. (1993). In vitro fusion of endocytic
771 vesicles is inhibited by cyclin A-cdc2 kinase. Mol Biol Cell *4*, 541-553.
772

Figure 1. Cyclin A2 accumulates in the cytoplasm at the S/G2 transition

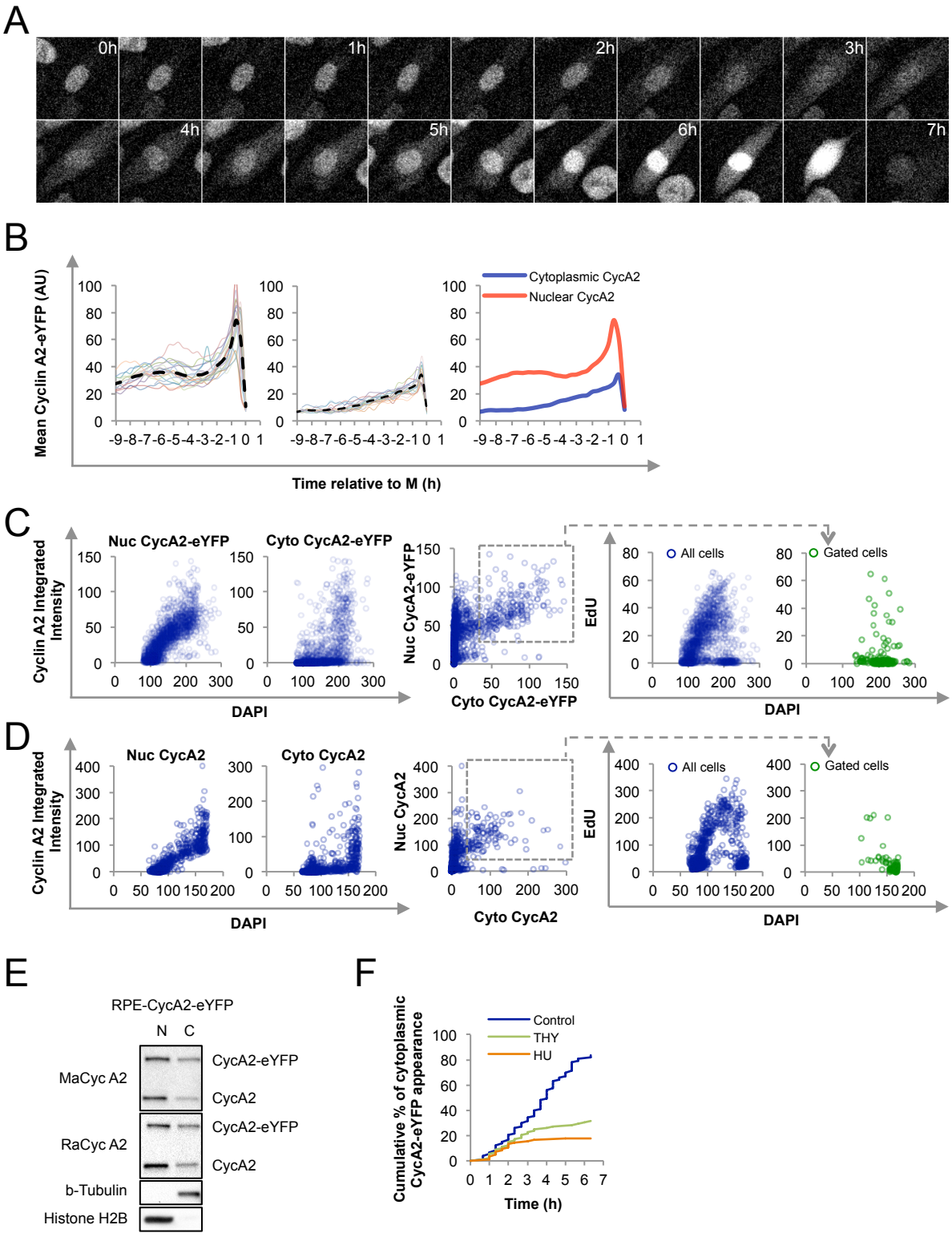

Figure 2. Cdk1 can contribute to cytoplasmic accumulation of Cyclin A2

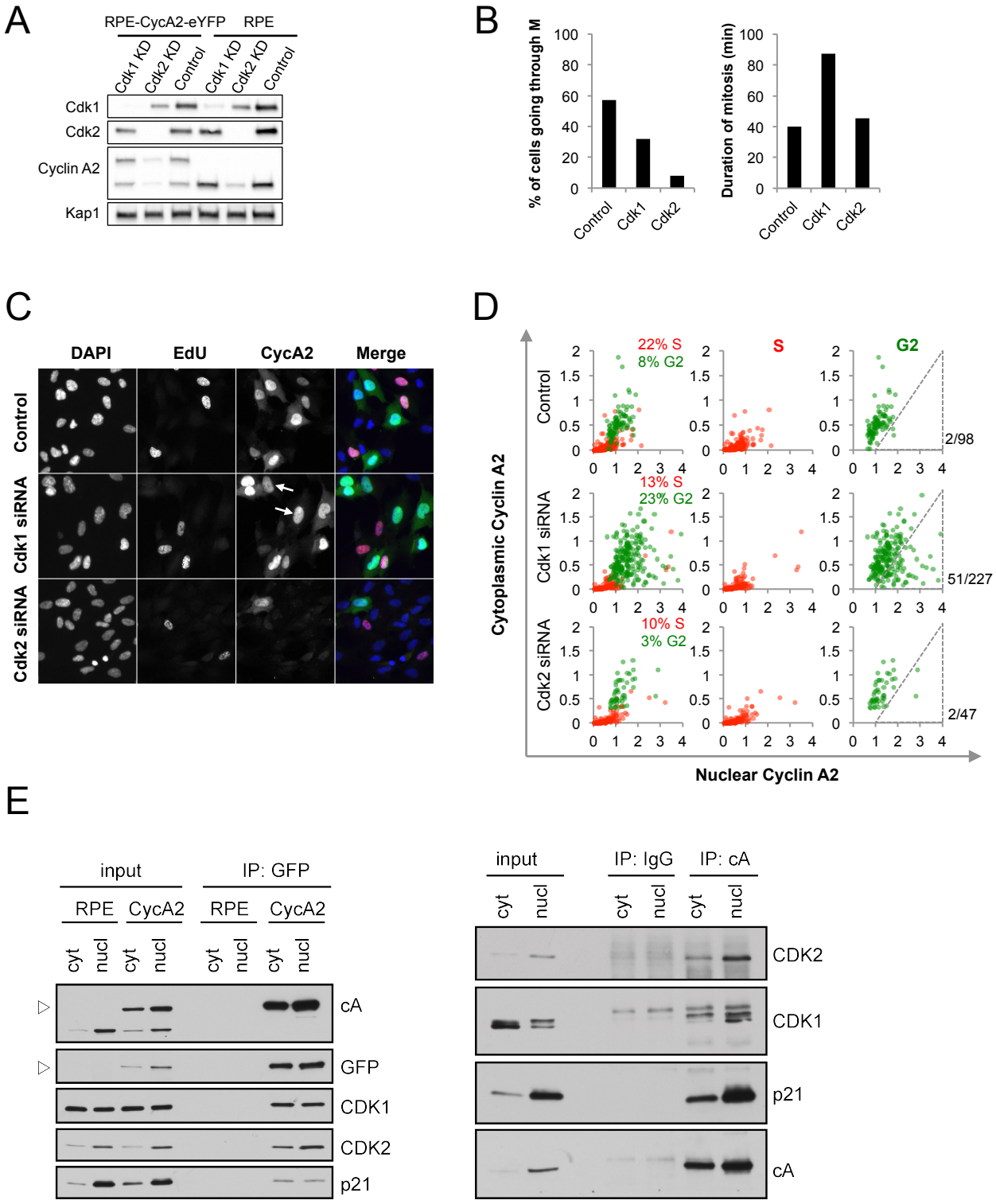

Figure 3. DNA damage and the DNA damage response can modulate cytoplasmic accumulation of Cyclin A2-eYFP

A

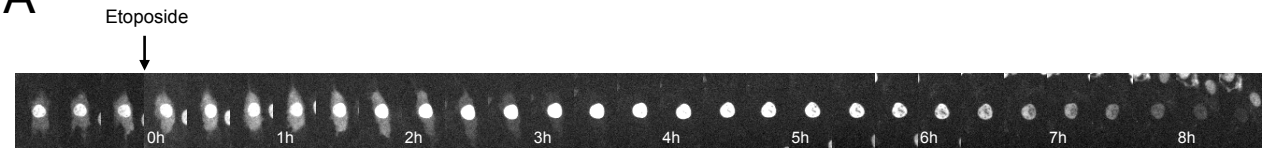

B

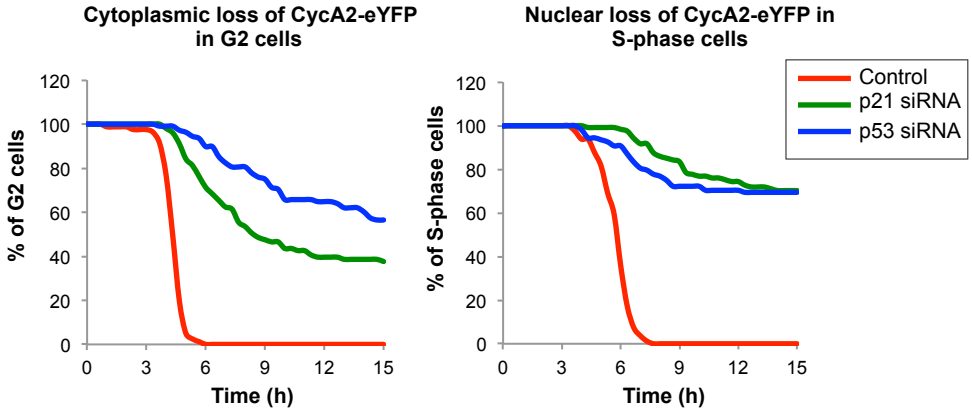

Figure 4. p21 can modulate Cyclin A2 localisation to the cytoplasm

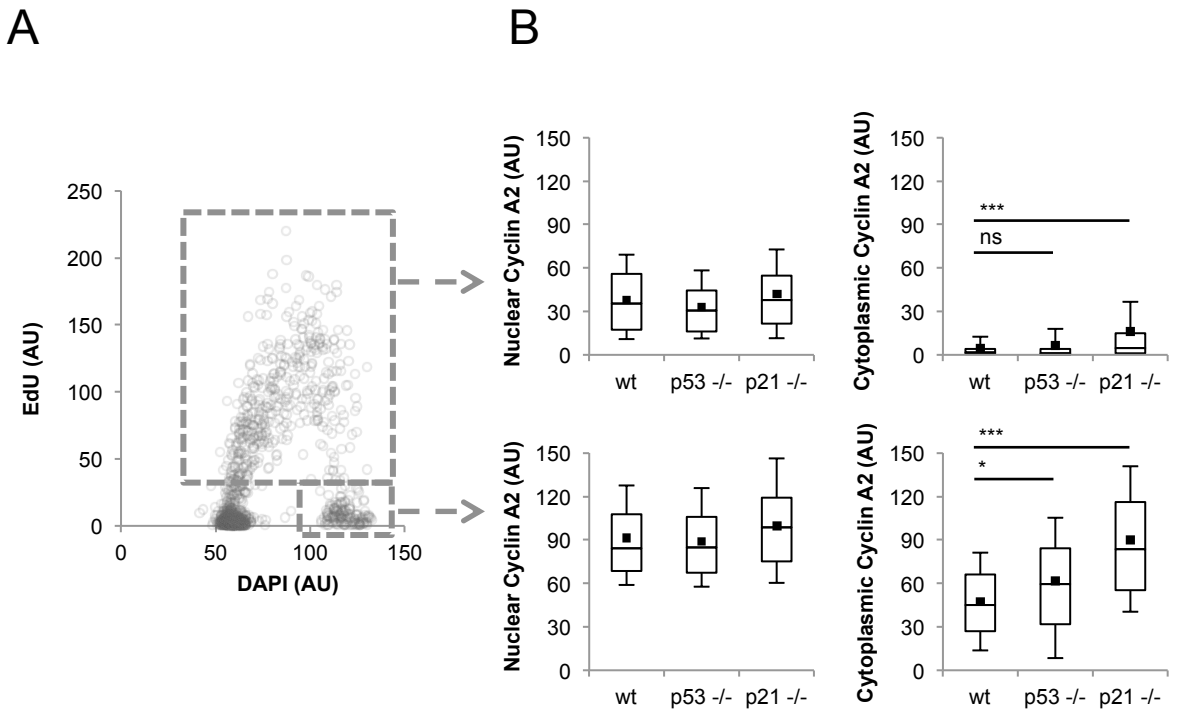

Figure 5. Cytoplasmic Cyclin A2 can activate Plk1

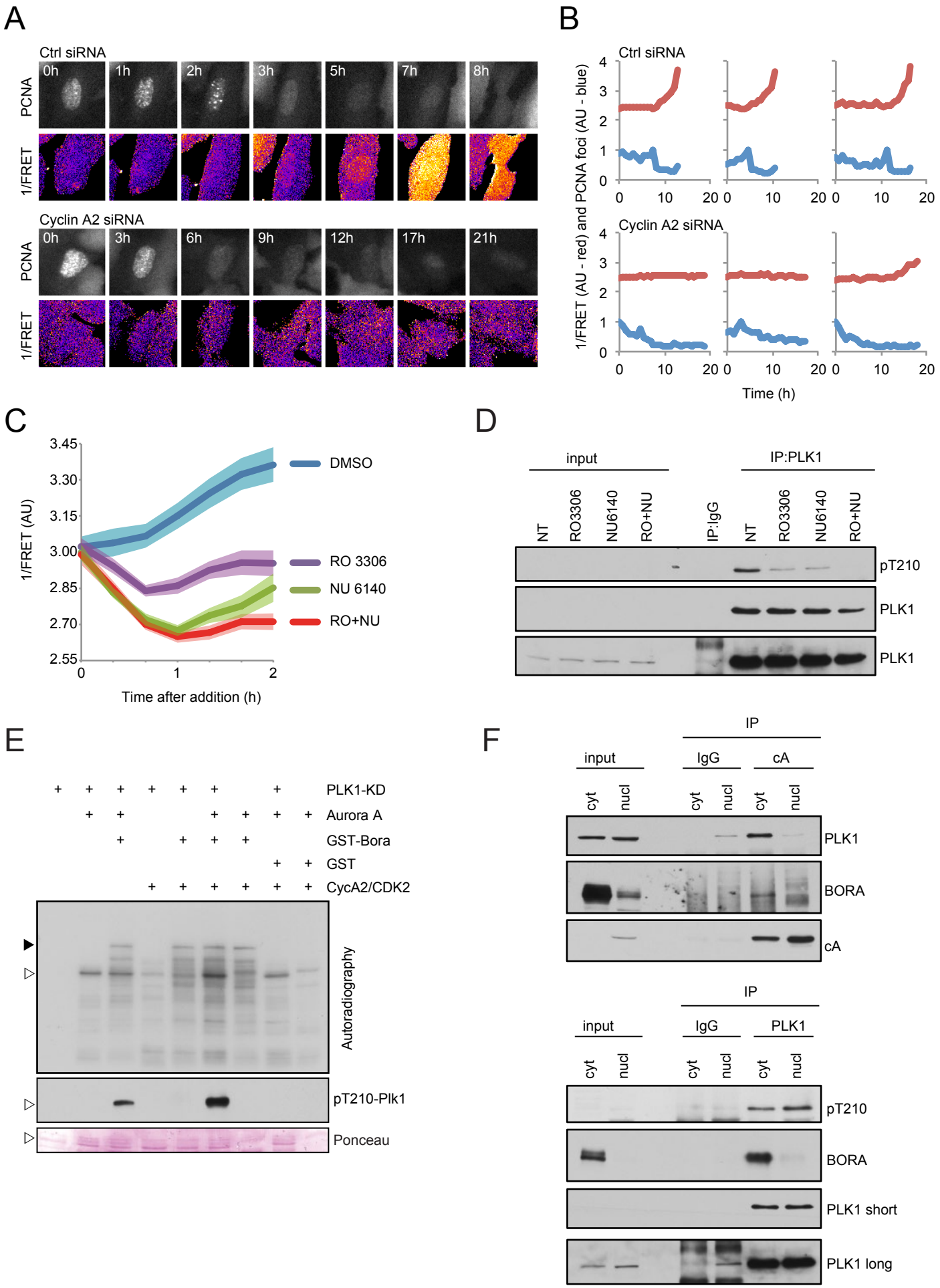

Figure 6. A model for Plk1 activation by cytoplasmic Cyclin A2

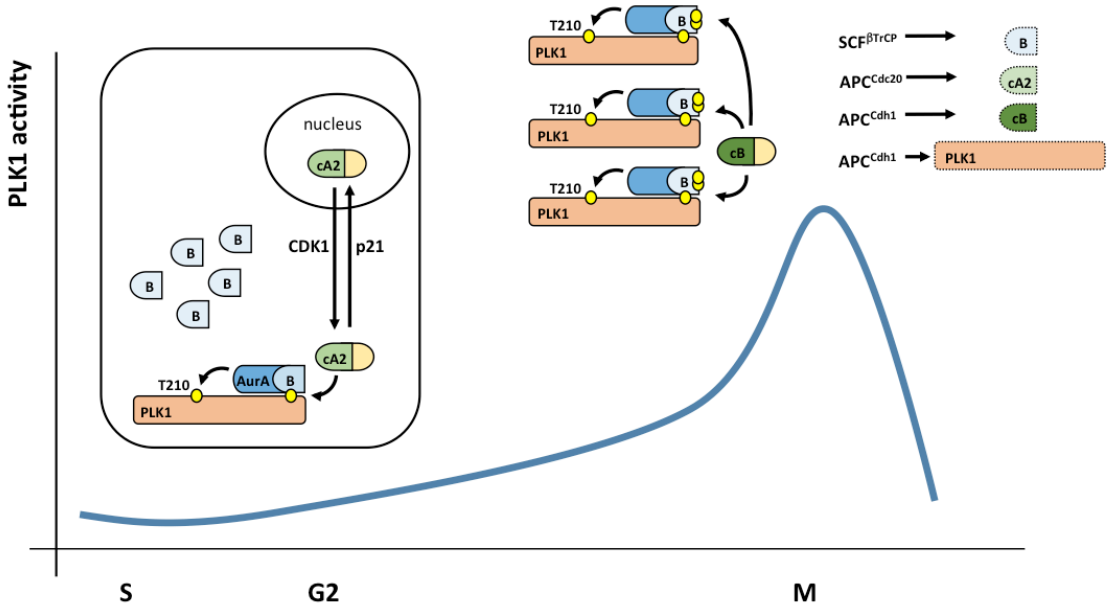

Supplementary Figure 1

A

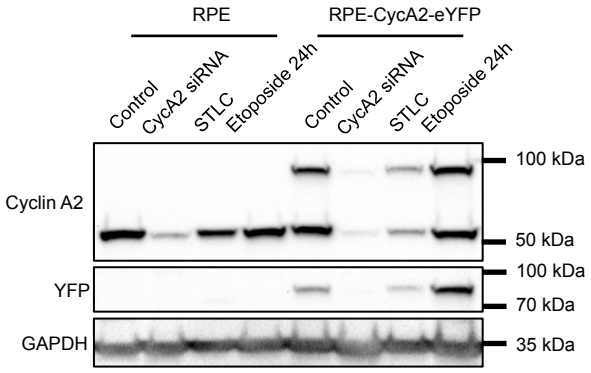

B

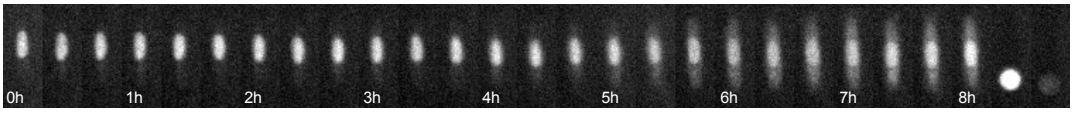

Supplementary Figure 2

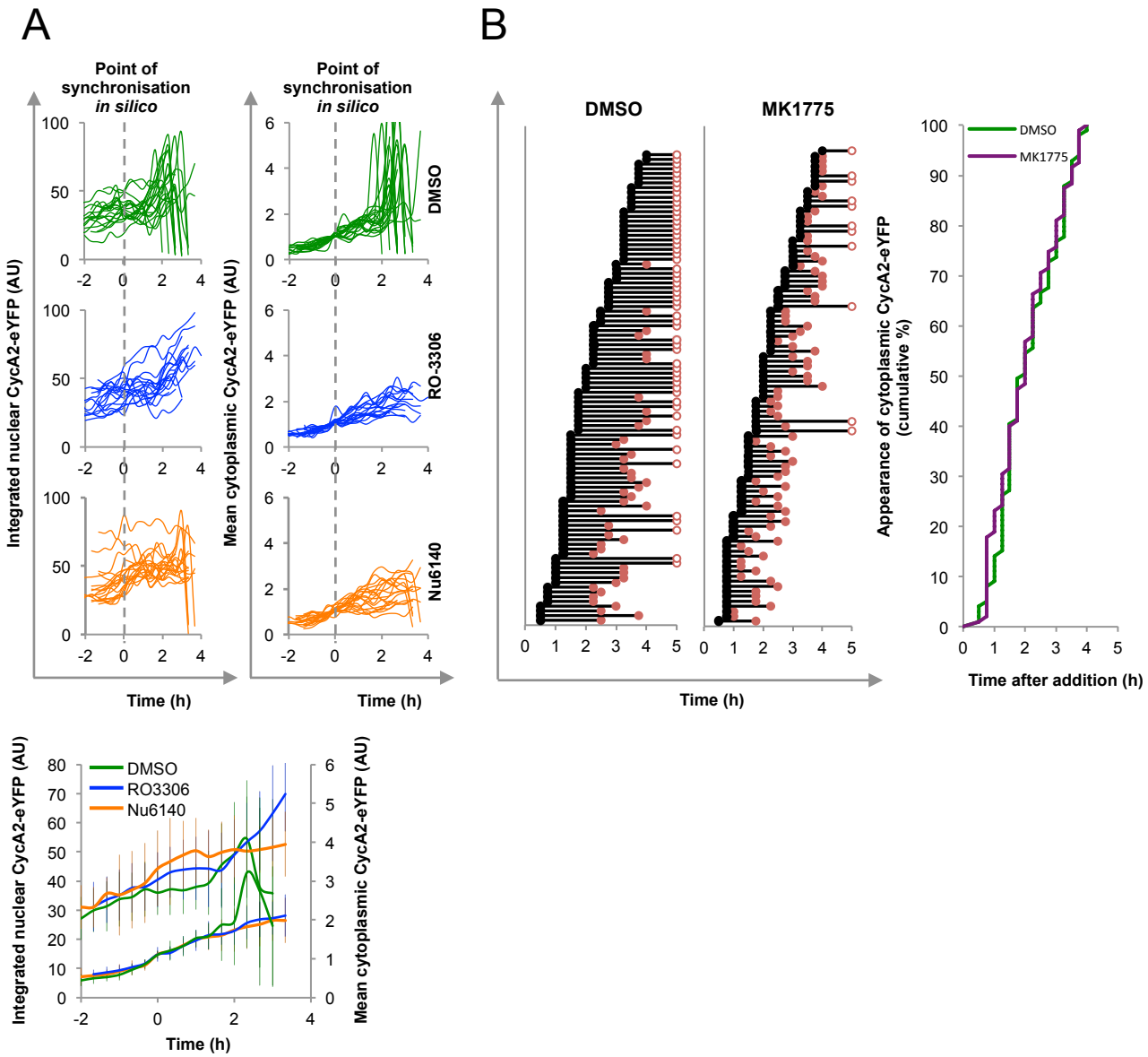

Supplementary Figure 3

A

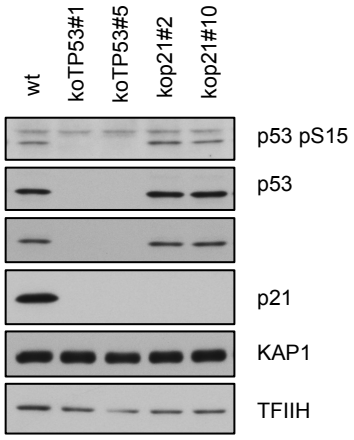

B

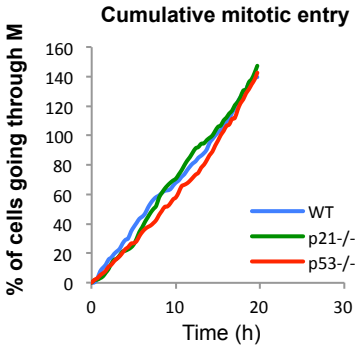
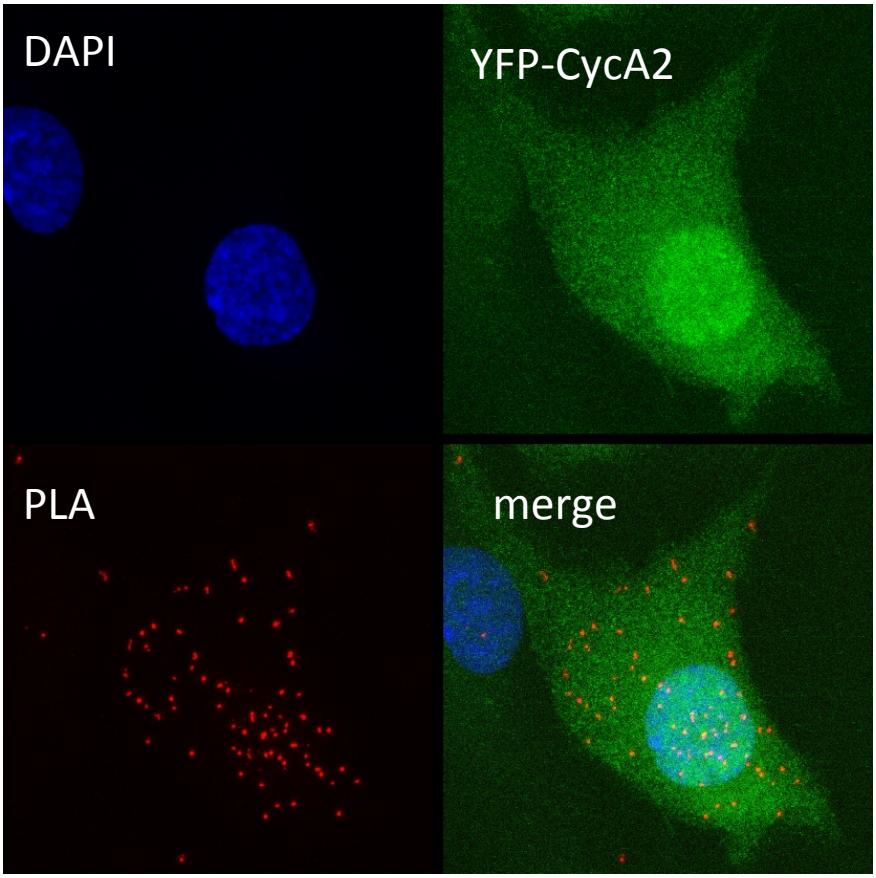
Supplementary Figure 4